TOWARDS FULL CHARACTERIZATION OF CONTINUOUS SYSTEMS IN TERMS OF PERIODIC ORBITS

Zbigniew Galias

Department of Electrical Engineering, AGH University of Science and Technology
al. Mickiewicza 30, 30-059 Kraków, Poland
e-mail: `galias@agh.edu.pl`, tel.: +48 12 6172890, fax: +48 12 6344825

ABSTRACT

In this work we describe a method to find for a continuous system all low–period cycles embedded within a numerically observed attractor. As an example of the application of this technique, we construct the trapping region for the Roessler system and find all periodic orbits of the associated Poincaré map up to period 11.

1. INTRODUCTION

It is well known that interval methods can be used to prove the existence of periodic orbits for discrete dynamical systems [1, 2]. It has also been applied to continuous systems with piecewise linear [3] and smooth [4] nonlinearities.

In this work, we describe a procedure that finds all short periodic orbits embedded within a chaotic attractor. The method consists of several steps. First a trapping region for the Poincaré map is found. This region is then covered by boxes. The image of each box is found and this information is used to construct the set of admissible connections. Next, we construct a set of periodic sequences of length n composed of admissible connections. For each sequence the interval operator is evaluated. In this way all period–n cycles enclosed in the trapping region are found.

In section 2 the method is described in detail, and in section 3 it is applied to the analysis of the Roessler system.

2. ANALYSIS OF CONTINUOUS SYSTEMS

Let us consider a continuous dynamical system defined by the set of ordinary differential equations

$$\frac{\mathrm{d}x}{\mathrm{d}t} = f(x), \qquad (1)$$

where $x \in \mathbb{R}^m$ and $f\colon \mathbb{R}^m \mapsto \mathbb{R}^m$ is a C^1 vector field.

This work was sponsored in part by KBN, grant no. 2P03A 041 24.

2.1. Poincaré map

As a first step of rigorous study, we reduce the continuous system (1) to the discrete one using the Poincaré map method. Let Σ be a hyperplane. The *Poincaré map* $P : \Sigma \mapsto \Sigma$ is defined as $P(x) = \varphi(\tau(x), x)$, where $\varphi(t, x)$ is the trajectory of (1) based at x, and $\tau(x)$ is the return time after which the trajectory $\varphi(t, x)$ returns to Σ. Periodic points of P correspond to periodic orbits of the continuous system.

2.2. Periodic orbits of the Poincaré map

The interval Newton operator [1] is defined as

$$\mathrm{N}(\mathbf{z}) = \hat{z} - F'(\mathbf{z})^{-1}F(\hat{z}), \qquad (2)$$

where $\mathbf{z}$ is an interval vector, $\hat{z} \in \mathbf{z}$, $F'(\mathbf{z})$ is the interval matrix containing $F'(z)$ for $z \in \mathbf{z}$. The most important property of the interval Newton operator states that if $\mathrm{N}(\mathbf{z}) \subset \mathbf{z}$, then F has exactly one zero in $\mathbf{z}$. On the other hand, if $\mathrm{N}(\mathbf{z}) \cap \mathbf{z} = \emptyset$, then there is no zeros of F in $\mathbf{z}$. These properties allow one to study rigorously the problem of the existence of zeros of F.

In order to find period–n orbits of P, we apply the interval Newton operator to the map $F : (\mathbb{R}^m)^n \mapsto (\mathbb{R}^m)^n$ defined by $[F(z)]_k = x_{(k \bmod n)+1} - P(x_k)$ for $k = 1, \ldots, n$, where $z = (x_1, \ldots, x_n)^{\mathrm{T}}$. Clearly, $F(z) = 0$ if and only if x_1 is a fixed point of P^n.

2.3. Evaluation of the Newton operator

For the rigorous evaluation of $P(\mathbf{x})$, we integrate equation (1) using the Lohner method, which helps to reduce the wrapping effect [5, 6]. The image of $\mathbf{x}$ under P is found as the intersection of Σ and the trajectory computed by the rigorous integration procedure.

In order to find $P'(\mathbf{x})$, we also need to solve the variational equation $\frac{\mathrm{d}D}{\mathrm{d}t} = \frac{\partial f}{\partial x}(x(t))D$, where $D(t, x_0) = \frac{\partial \varphi}{\partial x_0}(t, x_0)$ with the initial condition $D(0, x_0) = I$. Let $\mathbf{y}$ be the enclosure for the set $\{P(x)\colon x \in \mathbf{x}\}$, $\mathbf{D}$ be the enclosure for the solution of the variational equation $\{D(t,x) \colon x \in \mathbf{x}, t = \tau(x)\}$ and h be a vector orthogonal to Σ. The enclosure for the Jacobian matrix of P at $x \in \mathbf{x}$ can be found as

$$P'(\mathbf{x}) = \left(I - \frac{f(\mathbf{y}) h^T}{h^T f(\mathbf{y})} \right) \mathbf{D}. \tag{3}$$

For the details see [4].

2.4. Finding all periodic orbits of length n

In the first step of the procedure, we construct the trapping region for the Poincaré map. This region usually can be found by choosing a polygon enclosing trajectories of the Poincaré map generated by the computer.

In the second step, we cover the trapping region by boxes of a specified size. One option to find all periodic orbits is to apply the combination of the interval Newton method and a generalized bisection technique. This method works fine for discrete systems (see [2, 7]). For continuous systems, a better choice is to limit the number of interval vectors on which we need to evaluate the interval operator. To this end, we first find the graph representation of the dynamics of the system. We compute the image of each box and find the set of admissible transitions between boxes. Transitions represent edges of the directed graph. Once the graph representation is found, we reduce the graph by removing vertices corresponding to boxes having empty intersection with the invariant part of the trapping region. A box is removed if its image has empty intersection with other boxes or if it has empty intersection with images of all boxes. This procedure is continued until no more boxes can be removed. In this way, we can significantly reduce the size of the covering and hence the search space for periodic orbits.

Next, we find all period–n cycles in the graph. For each period–n cycle, we evaluate the interval operator on the corresponding interval vector $\mathbf{z}$ and check what is the position of $\mathrm{N}(\mathbf{z})$ with respect to $\mathbf{z}$. If $\mathbf{z} \cap \mathrm{N}(\mathbf{z}) = \emptyset$, then there is no period–n orbits in $\mathbf{z}$. If $\mathrm{N}(\mathbf{z}) \subset \mathbf{z}$, then there exists exactly one period–n orbit inside $\mathbf{z}$. If neither of these two conditions hold, then one option is to divide the interval vector $\mathbf{z}$ into smaller parts and to evaluate the interval operator on each of them. For long orbits, this leads to many divisions and a long computation time (for example, for $n = 10$ and the dimension of a Poincaré map equal to 2, we should search the space of dimension 20). This is not feasible and we choose a different method.

There are two reasons that neither of the two conditions may be fulfilled. One is that the position of the orbit is too close to the border of $\mathbf{z}$. In this case, we try to proceed by increasing the size of $\mathbf{z}$. Namely, we set the new value of $\mathbf{z}$ to be the convex hull of $\mathbf{z}$ and $(1+\varepsilon)\,\mathrm{N}(\mathbf{z}) - \varepsilon\,\mathrm{N}(\mathbf{z})$. In many cases this technique allows one to find a periodic orbit in $\mathbf{z}$. The second reason may be that the diameter of $\mathrm{N}(\mathbf{z})$ is larger than the diameter of $\mathbf{z}$. In this case, we should use a bisection technique, but as mentioned before this usually will not work due to the size of the search space. In such a case we stop the computations and try again with a finer grid.

The computation time depends on the number of period–n cycles in the graph. One way to reduce this number is to find the cycles of the graph for a finer division, and then to construct the graph for a division with boxes two (or more) times larger in each direction.

3. NONLINEAR SYSTEM

As an example, we consider the Roessler system

$$\frac{\mathrm{d}}{\mathrm{d}t} \begin{pmatrix} x_1 \\ x_2 \\ x_3 \end{pmatrix} = \begin{pmatrix} -x_2 - x_3 \\ x_1 + a x_2 \\ b + x_3(x_1 - c) \end{pmatrix}. \tag{4}$$

We consider the system with the parameter values $a = 0.2$, $b = 0.2$, $c = 5.7$. A typical trajectory is shown in Fig. 1.

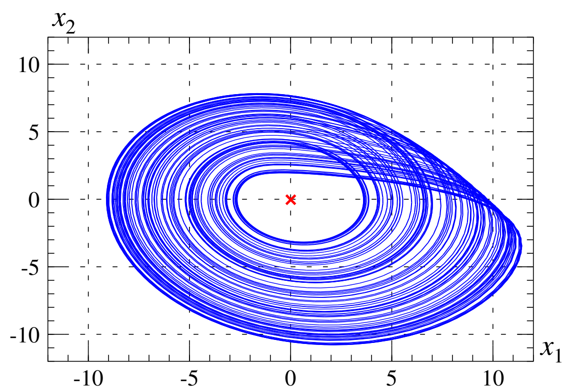

Fig. 1. Roessler attractor

In order to apply the methods described previously, we choose a Poincaré map P defined by the hyperplane $\Sigma = \{x \in \mathbb{R}^3 \colon x_1 = 0,\, \dot{x}_1 > 0\}$.

3.1. The existence of the trapping region

In order to construct a trapping region for P, we first plot a trajectory of P (see Fig. 2). Next we choose a region R enclosing the computer generated trajectory and check rigorously whether its image is enclosed in itself ($P(R) \subset R$). It should be noted that once we

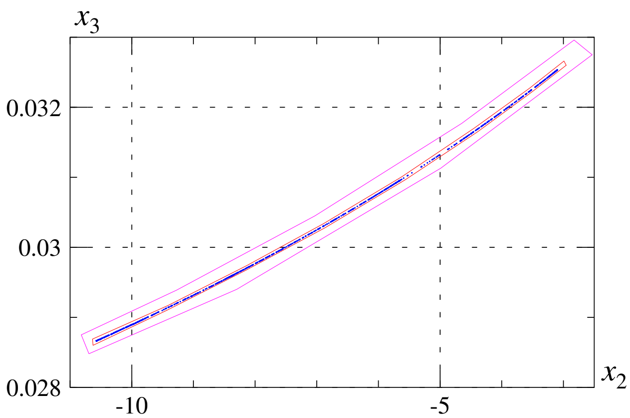

Fig. 2. Trajectory of the Poincaré map and two trapping regions.

know that the Poincaré map is well defined on R, it is sufficient to check the enclosure condition ($P(x) \in R$) only at the border of R. Two examples of polygons being trapping regions for the map P are shown in Fig. 2. In order to prove the enclosure condition for the larger polygon we cover its border by 504 rectangles, evaluate the Poincaré map on each of these rectangles, and check that the images are enclosed in R. For the smaller set we needed to cover the border by 8422 rectangles to complete the proof.

The small trapping region has the advantage that further study can be reduced to a smaller set, and hence the computation time can be significantly shorter.

3.2. Generation of the graph

In the second step of the analysis, we cover the trapping region by rectangles of the same size, find the image of each rectangle, and construct the set of admissible transitions between rectangles. Using the method described in section 2 we remove boxes lying outside the invariant part of the trapping region.

box size	b	c
0.0125×0.000025	1675	8355
0.00625×0.0000125	2808	12323
$0.003125 \times 0.00000625$	5258	22052
$0.0015625 \times 0.000003125$	10477	43681
$0.00078125 \times 0.000001562$	22416	96594

Table 1. Covering of the trapping region; b represents the number of boxes and c the number of admissible connections.

In Table 1 we report the number of boxes and admissible connections for different box sizes. To see that the reduction of the graph is an important step of the analysis, let us note that for the boxes of size $0.003125 \times 0.00000625$, there are 31722 boxes with 138821 connections before the reduction, and only 5258 boxes with 22052 connections after it.

3.3. Periodic orbits

Next, we find in the graph all cycles of a specified length. For each cycle, we generate a sequence of interval vectors and evaluate the interval operator on this sequence. In this way, we were able to find all periodic orbits up to period 11 (see Fig. 3).

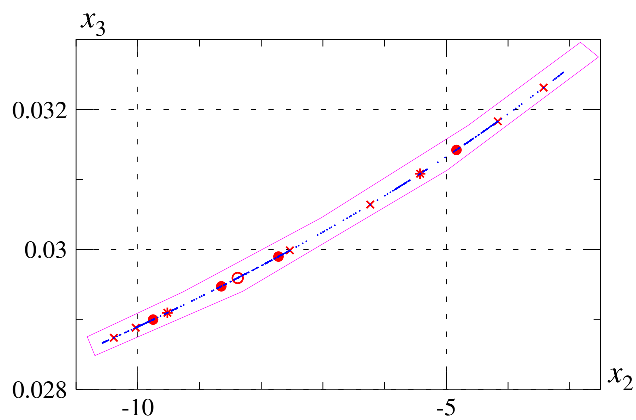

Fig. 3. Periodic orbits of P with period $n \leq 11$: fixed point ($\circ$), period–2 orbit ($\ast$), two period–3 orbits ($\times$), period–4 orbit ($\bullet$).

In table 2, we report the number Q_n of periodic orbits with period n, the number P_n of fixed points of P^n, and certain computation details.

n	Q_n	P_n	C_n	T_n	time [s]
1	1	1	1	1	0.19
2	1	3	2	2	0.72
3	2	7	4	19	10.00
4	1	7	6	11	7.79
5	2	11	7	32	28.24
6	3	27	40	140	147.31
7	4	29	29	139	171.59
8	7	63	42	115	162.10
9	10	97	109	704	1116.05
10	15	163	1055	2381	5835.80
11	24	265	713	2802	7964.30

Table 2. Periodic orbits of P; Q_n is the number of period–n cycles, P_n is the number of fixed points of P^n, C_n is the number of period–n cycles in the graph, T_n is the number of evaluations of the interval operator.

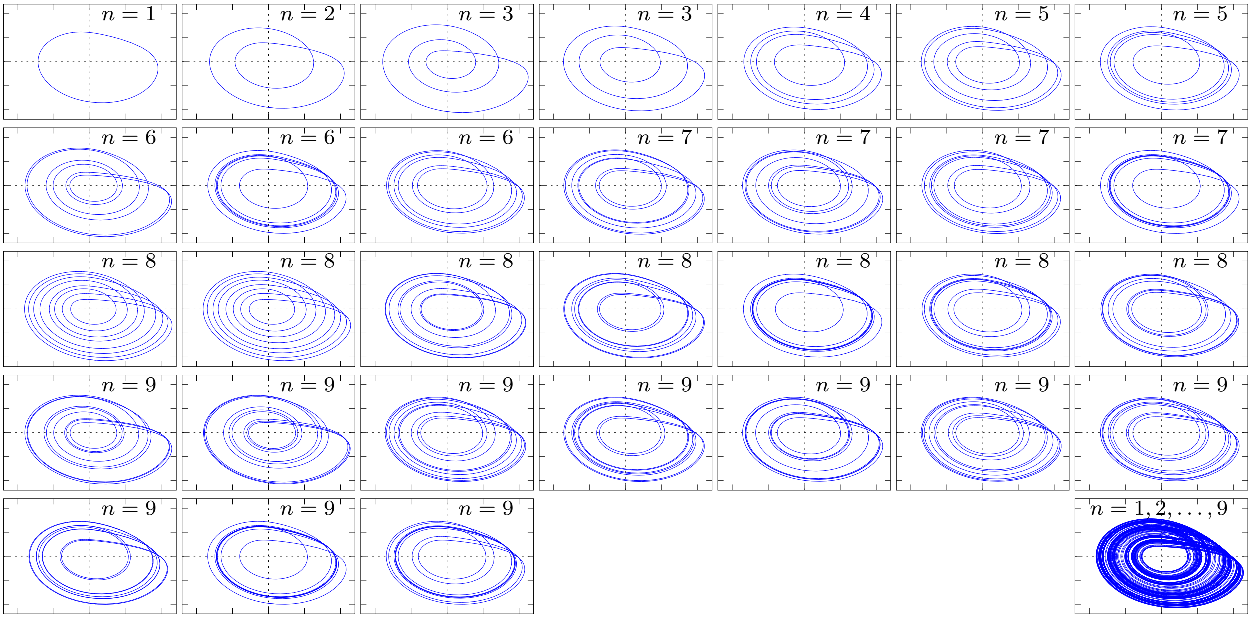

Fig. 4. All periodic orbits of the Roessler system with period $n \leq 9$.

The computations for $n \leq 9$ were done for the box size of $0.0015625 \times 0.000003125$. After finding period–$n$ cycles in the graph, the number of cycles was reduced by increasing the grid size to 0.0125×0.000025 (8 times). For example, for $n = 8$ we have found 21655 period–8 cycles and after increasing the grid size this number was reduced to 42 (see Table 2). It is interesting to note that the number of period–8 cycles for the grid size of 0.0125×0.000025 is 114106.

For the box size of $0.0015625 \times 0.000003125$ and $n = 10$ the procedure was unsuccessful. To avoid the large number of divisions in the bisection method, we used a finer grid of $0.00078125 \times 0.000001562$.

Periodic orbits of the continuous system corresponding to periodic orbits of P with period $n \leq 9$ are shown in Fig. 4.

4. CONCLUSIONS

In this work, we have described a general method for finding in a given region all low–period cycles for continuous systems. The method works under the assumption that the Poincaré map is well defined and continuous on this region. If the region encloses the attractor, we can claim that all periodic orbits embedded within the attractor are found.

The method can be applied without any modifications for higher dimensional systems. In such a case, due to the necessity of searching a higher dimnesional space computation times may be significantly larger.

5. REFERENCES

[1] A. Neumaier, *Interval methods for systems of equations*, Cambridge University Press, 1990.

[2] Z. Galias, "Interval methods for rigorous investigations of periodic orbits," *Int. J. Bifurcation and Chaos*, vol. 11, no. 9, pp. 2427–2450, 2001.

[3] Z. Galias, "Proving the existence of periodic solutions using global interval Newton method," in *Proc. IEEE Int. Symposium on Circuits and Systems, ISCAS'99*, Orlando, 1999, vol. VI, pp. 294–297.

[4] Z. Galias, "Periodic orbits for an electronic circuit with a smooth nonlinearity," in *Proc. European Conference on Circuit Theory and Design, ECCTD'03*, Kraków, 2003, vol. I, pp. 205–208.

[5] R. Lohner, "Computation of guaranteed enclosures for the solutions of ordinary initial and boundary value problems," in *Computational ordinary differential equations*, J.R. Cash and I. Gladwell, Eds. Clarendon Press, Oxford, 1992.

[6] R.E. Moore, *Interval Analysis*, Prentice Hall, Englewood Cliffs, NJ, 1966.

[7] Z. Galias, "Rigorous investigations of Ikeda map by means of interval arithmetic," *Nonlinearity*, vol. 15, pp. 1759–1779, 2002.